Egypt.J.Chem. **Vol. 63**, No. 5. pp. 1585 - 1603 (2020)

Egyptian Journal of Chemistry
http://ejchem.journals.ekb.eg/

Evaluation of Montmorillonite (MMT)/polymer Nanocomposite in Gap Filling of Archaeological Bones

G. Abdel-Maksoud[1], R. A. Sobh[2]*, A. Tarek[3], S.H. Samaha[4]

[1]*Conservation Department, Faculty of Archaeology, Cairo University, Giza, Egypt*
[2]*Polymer and Pigment Department, National Research Centre, Dokki, Giza, Egypt*
[3]*Conservation Centre, Grand Egyptian Museum, Ministry of Antiquities, Egypt*
[4]*Textile Metrology Department, National Institute for Standards, Tersa Street, Giza, Egypt*

ARCHAEOLOGICAL bones are exposed to various deterioration factors, so polymers are used to improve their properties and give more durability. Traditional pastes were applied and evaluated before. This study aims to evaluate some modified pastes in order to improve the properties of traditional pastes. Montmorillonite MMT was modified with amino acid and characterized in terms of Fourier Transform Infrared Spectroscopy (FTIR), X-Ray Diffraction XRD and scanning electron microscope SEM. Nanocomposites of modified MMT with paraloid as acrylic polymer were evaluated using XRD to be used for gap filling and completion of archeological bones to give more resistance against surrounding environmental conditions.

Accelerated ageing were used for evaluation of modified pastes and estimated through change of color by UV spectrophotometer, FTIR, mechanical properties (tensile, elongation and compressive strength) and surface morphology by SEM.

The results confirmed that the modified pastes with modified mMMT nanocomposite showed good resistance against thermal ageing, and give high stability in terms of color change value, surface morphology and mechanical properties. As pastes with the mMMT gave negligible color difference as 0.98. In addition, the contact angles measurements reduced with smaller ratios as 12% and 7.5% than their corresponding pastes with no mMMT 22% and 11%, respectively. Moreover, pastes with mMMT showed higher density, lower porosity and lower water absorption and exhibit more resistance against thermal ageing.

Keywords: Archaeological bone, Clay/polymer nanocomposite, Physico-mechanical roperties

Introduction

Polymer nanocomposite is a composite material comprising a polymer matrix and an inorganic dispersive phase that is nanometric in scale (≤100 nm). Applying nanomaterial with nanoscale size permit to create high performance materials with novel properties and be compatible with other materials. So, these have gained tremendous attention to overcome the imitations of polymeric materials by preparing suitable nanocomposites with their superiority, excellent barrier properties, reinforcement of mechanical performance [1]. Nanoclay is one of silicon-based nanomaterials with a layer structure. The most common of which is montmorillonite MMT, hydrated Sodium Calcium Aluminum Magnesium Silicate Hydroxide (Na, Ca) (Al, Mg)$_6$ (Si_4O_{10})$_3$(OH)$_6$-nH2O [2-5].

Montmorillonite MMT was selected to be used with the polymers as nanocomposites and form interfacial bonding between polymer and nanoclay to improve the polymer performance in terms of rheological and physico-mechanical properties (elasticity, toughness) at high

*Corresponding author e-mail: rokaya_aly@yahoo.com
Received 19/9/2019; Accepted 16/10/2019
DOI: 10.21608/ejchem.2019.15761.2051

temperature and control over ageing resistance. Due to the nanoscale dispersion and the high aspect ratios of the clays, polymer-layered silicate nanocomposites exhibit light weight, good dimensional stability, high heat resistance, high stiffness, high barrier properties, and improved fracture toughness and tensile strength [6-11].

The MMT/polymer nanocomposite can be synthesized through various preparation methods including in-situ template synthesis, solution intercalation, in-situ intercalative polymerization and melt intercalation. We used in this paper the solution intercalation method. Simply, it involves dissolving the polymer in a solvent and the clay is dispersed in the same solution by the aid of sonication and the polymer chains intercalate between the layers. The intercalated nanocomposite is obtained by solvent removal through vaporization or precipitation [12].

On the other hand, bone composition consists of organic material, collagen, non-collagenous protein, lipids and carbohydrates in addition to inorganic mineral as calcium hydroxyapatite $Ca_{10}(PO_4)_6(OH)_2$. Although its composition varies considerably with age and type of bone. Moreover, when bones are removed from the body they become unstable because they are moved from a relatively closed environment to an open one and can be broken down over time through physical breaking, decalcification and dissolution due to acidic soil and water [13-16].

The deterioration of the archaeological bone may occur as a result of weathering, fracturing, cracking, surface marks, microbial attack, abrasion, polishing and breakage and these factors occur in isolation or in combination [17, 18]. So the preservation of bone depends not on the length of time has been underground, but the type of bone and burial environment [19].

Examples of the polymer almost used in traditional pastes are polyvinyl acetate (PVA), paraloid B72 (ethyl methacrylate copolymer) , polyvinyl acetate (PVA) emulsions, and in some cases Elmer's Glue is suitable for the completion of missed parts in bones[20]. Stollman tested a mixture of glass micro-balloons and Paraloid B72 dissolved in acetone for filling the missing parts of blue whale skeleton [21].

The current article is concerned in modification of montmorillonite mMMT with amino acid and its using with paraloid B72, B82 as acrylic polymers to form MMT/paraloid nanocomposite. Then, studying the effect of applying these nanocomposites to improve the resistance of pastes that used in gap filling and completion the missing parts of archaeological bones against surrounding environmental conditions in terms of physico- chemical and optical properties.

Materials &Methods

Materials

Montmorillonite MMT (with CEC 92 mg.eq) was from southern clay products, inc., Gonzales, Texas. Paraloid B 72, paraloid B 82, calcium carbonate and glass micro-ballons were purchased from Rohm and Haas Co., USA. Hydrochloric acid was from Sigma-Aldrich-Germany. Xylene were from ADWIC- El Nasr pharmaceutical chemicals co- Egypt. L (+)-Asparagine amino acid AA was purchased from Pour biochimie-MERCK eurolab, made in CE.

Preparation of MMT/polymer nanocomposites

Intercalated modification of MMT with amino acid:

Montmorillonite MMT clay was modified with amino acid to organophilic clay. MMT (2.5 g) was dispersed in 250 ml distilled water for stirring for 1 h and then heated to 70 ^{o}C to obtain aqueous suspension of clay. The desired amount of L (+)-Asparagine amino acid AA (0.5 gm) (2x concentrations of the clay based on CEC) dissolved in 50 ml distilled water and 2 ml of hydrochloric acid was added into the mixture then stirring was continued for 4 h. The modified clay as a white precipitate was filtered and washed with distilled water. The obtained wet precipitate was dried in oven under vacuum at 80 ^{o}C for 24 h [22].

Preparation of MMT/polymer nanocomposites by solution method:

The weighed amount of modified MMT clay (1% of polymer) was suspended in 20 ml of xylene using ultrasonic apparatus. MMT suspension was mixed with solution of the polymer either paraloid 72 or paraloid 82 in xylene (with concentration of 15%) at a temperature of 80 ^{o}C and stirred for 2hr using magnetic stirrer at 500 rpm. MMT/polymer nanocomposites solution became ready to be applied [23].

Preparation of pastes

Pastes no. 1, 2: consist of nanocomposites modified montmorillonite mMMT/ paraloid B72; which was used as adhesive; and filler as calcium carbonate $CaCO_3$ or glass microballoons was added to adhesive in ratio 1:1 and 1:3 in pastes 1 and 2, respectively.

Pastes no. 3, 4: consist of paraloid B 82 which was used as adhesive; and filler as calcium carbonate $CaCO_3$ or glass microballoons was added polymer in ratio 1:1 and 1:3 in pastes 3 and 4, respectively.

Pastes no. 5, 6: consist of nanocomposites mMMT/ paraloid B 82; as adhesive; and filler as calcium carbonate $CaCO_3$ or glass microballoons in ratio 1:1 and 1:3 in pastes 3 and 4, respectively.

Pastes were prepared at room temperature. A stainless template was made to mold pastes, and the size of samples were adjusted as 10 cm length × 2 cm width × 0.5 cm thickness. Pastes were left for a week to dry at room temperature.

Thermal ageing

The prepared pastes were placed in an oven (PID system, Type: M 120 - VN). Pastes were exposed to thermal ageing at 100°C for various ageing time from 1 day to 8 days [24, 25].

Investigation Methods

Change of color by spectrophotometer

Color changes of the studied samples were measured by spectrophotometer Optimatch 3100model, from the SDL Company. The dimension of the measured area of each sample was (1x1) cm^2. The total color difference ΔE* between two color stimuli $\Delta E^* = \{(\Delta L^*)^2 + (\Delta a^*)^2 + (\Delta b^*)^2\}^{1/2}$ [26, 27]. Where the colors are given in CIE Lab coordinates, L* corresponding to the brightness (100 = white, 0 = black), a* to the red–green coordinate (positive sign = red, negative sign = green), and b* to the yellow–blue coordinate (positive sign = yellow, negative sign = blue).

Fourier Transform Infrared Spectroscopy (FTIR)

The changes of pastes samples before and after ageing were determined by using FTIR spectrophotometer (JASCO-FT/IR-6100) in the range of 4000–400 cm^{-1} using KBr powder.

Each sample was mixed with KBr and placed in a Drift cell [28]. FTIR Spectra were assigned for samples (standard (0 day) & after heat ageing (8 days)) from each paste.

Tensile and elongation measurements:

Tensile strength and elongation were determined by using an electronic tensile testing machine (Zwick 1425) and was calculated by using the following equation: Tensile strength (T.S) = (F/t.w) MPa, Where F= load applied to rupture, t= the thickness of the specimen and w= width of the specimen. Load cell: 500MPa and the Cross head speed: 100mm/min.

At the break, the elongation

n is expressed as the percent of the original bench mark length attained beyond rupture. Ultimate elongation E % = ((L-L0)/ L0) 100, Where: L = Length of the specimen at the moment of rupture and L0= the length between bench marks accordingly to ASTM, D 412-66 T [29, 30].

Compressive strength

Measurement of compressive strength was taken by the TINIUS OLSEN H5KT dynamometer, accordingly to ISO 2062 standard. Load cell: 250MPa and the Cross head speed: 200mm/min [31].

Investigation of the surface morphology by a scanning electron microscope SEM:

The surface morphology of the pastes samples studied were examined by scanning electron microscope (SEM) using a QUANTA FEG250 model- Japan. All samples were conditioned under the standard atmospheric conditions for 24 hours [32].

X-Ray Diffraction (XRD)

X-ray diffraction patterns of model (XPERT – PRO – PANalytical – Netherland) ;using a diffract meter equipped with a rotating target X-ray tube and a wide-angle goniometer. The X-ray source was Ka radiation from a copper target with graphite monochromater. The X-ray tube was operated at a potential of 45 kV and a current of 40 mA. The range (2hr) of scans was performed

from 10 °C to 80 °C at a speed of 4° per minute at increments of 0.05° [13].

Density, porosity and water absorption

The measurement of water absorption, porosity and density were attempted in accordance with Al-Dosari et al. [33, 34], the size of the samples was 2cm (length)×2cm (width)×0.5cm (thickness). Tests were carried out on samples before and after heat ageing. The samples were completely immersed in deionized water at room temperature. After 24h, the samples were taken out, wiped with tissue paper carefully and weighed immediately.

Density was measured as weight (g) over volume (cc) with volume determined by displacement according to the equation [35]**:**

$$\text{Density} = W/V = \ldots \text{ g/cm}^3$$

where W is the sample weight and V is the sample volume.

Porosity was measured according to the equation [35]

$$\text{Porosity} = W_2 - W_1 / V \times 100 = \ldots \%$$

where, W_1 is the mass of the sample before immersion, W_2 is the mass of the sample after immersion in water for 24h and V is sample volume.

Water absorption measurements were carried out according to (UNI 10859, 2000) [36] according to the equation: [37]

$$\text{Water absorption} = W_2 - W_1 / W_1 \times 100 = \ldots \%$$

where, W_1 is the mass of the sample before immersion and W_2 is the mass of the sample after immersion in water for 24h.

Contact angle measurement (wettability)

Contact angle of pastes samples was determined by SDL image analysis high resolution video camera microscope and the sample was put on a leveled stage. 5µl distilled water was applied on the sample. The image of the water droplet was captured. After the imaging process, the contour was applied to fit the water droplet. The tangent at the point of contact between the water droplet contour and surface of the sample was drawn and the inner angle of the tangent and the sample surface was measured manually using protractor [31].

Results and Discussions

Intercalated modification of MMT

To have a homogeneous dispersion in hydrophobic polymer matrix, the hydrophilicity of Montmorillonite MMT was decreased through ion-exchange reactions using L (+)-Asparagine amino acid, which, in turn, lower the hydrophilicity of the silicate surface and also increase the interlayer distance. The reaction process was carried out at a temperature of 70°C for 90 minutes in a batch reactor equipped with a magnetic stirrer rotating at a speed of 300 rpm. The amino acid treated MMT was collected as a white ppt and dried under vacuum. This intercalation could be confirmed by IR-spectra, X-ray diffraction and scanning electronic microscope SEM.

The FT-IR spectra for each of the L (+)-Asparagine amino acid, neat MMT and the modified MMT (AA treated MMT) is represented in Figure 1. The IR spectra for the neat MMT sample showed its absorbance at various wave numbers. At 3600 cm^{-1} band, the peaks for both neat and modified MMT samples 2, 3 are the same. But within 1600 to 3000 cm^{-1} band region, the peaks are well pronounced on the amino acid treated MMT while such peaks are not found in untreated MMT spectra.

The XRD patterns of neat MMT and modified MMT are illustrated in Figure 2 and it is observed that XRD of the neat MMT shows a diffraction peak at about $2\Theta = 6.5064$, corresponding to a d-spacing of 13.5 nm. The data for d-spacing are listed in (Table 1) which shows that the diffraction peaks of the modified MMT sample are shifted to smaller angel and the d-spacing increased compared with the neat MMT. This indicates that mMMT was successfully intercalated homogeneously with L (+)-Asparagine amino acid [38].

The transformation in surface morphology of both of the neat MMT and modified MMT was examined by scanning electron microscope SEM and their images are represented in Figure 3. The SEM images showed an obvious surface morphology transformation and interlayer spacing that confirm the successful intercalation of MMT by the amino acid and increasing the space between layers.

MMT/polymer nanocomposite:

The weighed amount of modified MMT

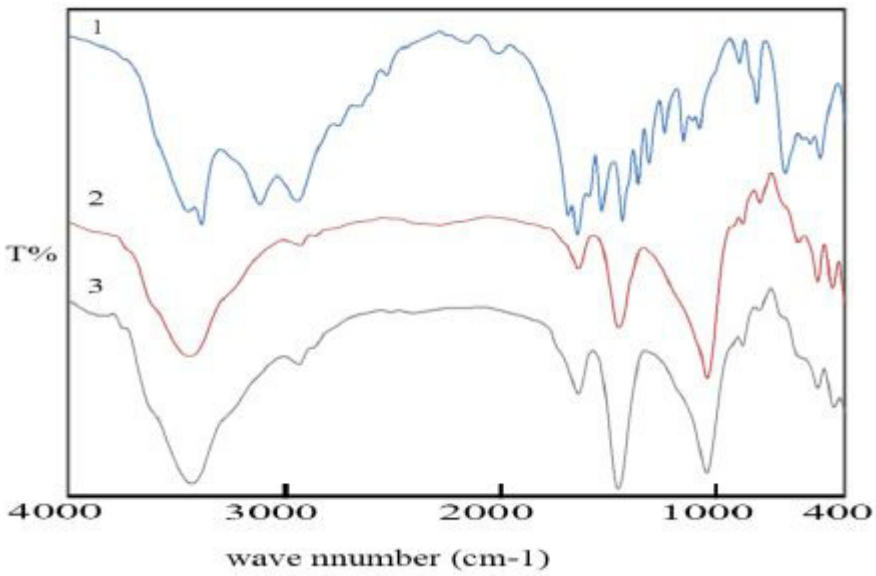

Figure 1: FT-IR Spectra of Amino acid (1) neat MMT (2) and modified MMT (3).

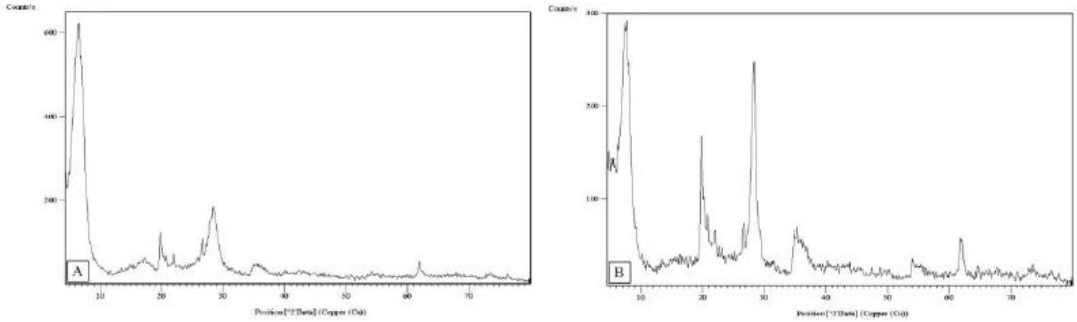

Figure 2: XR diffraction patterns for the neat MMT clay (A) and modified MMT clay (B)

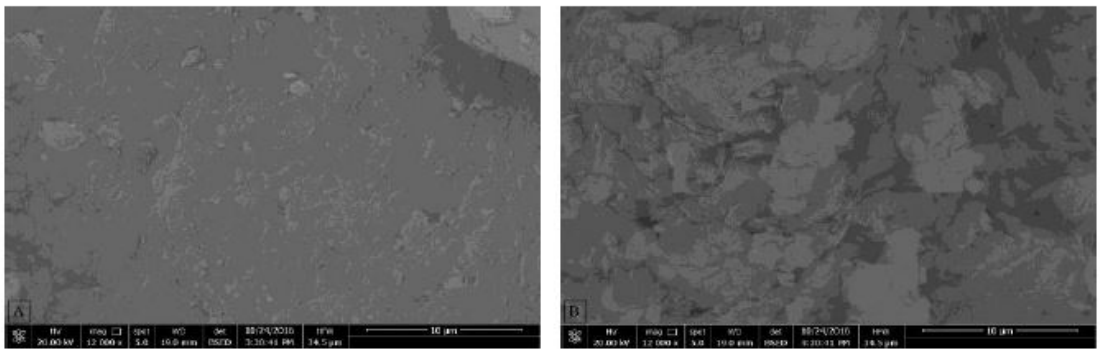

Figure 3: SEM of the neat MMT (A) and the modified MMT (B)

was suspended in solution of the polymer either Paraloid 72 or Paraloid 82 in xylene solvent at a temperature of 80 °C and stirred for 2hour to form MMT/polymer nanocomposite. The nanocomposite formation was proved by X-ray diffraction in Figure 4 that shows XRD patterns for the MMT composites with both of Paraloid 72 and Paraloid 82. It could be observed the absence of any sharp crystalline peak that characterize the MMT indicating homogenous dispersion in the composite which refer the formation of amorphous complex [39]. From XRD results, it could be concluded that the inter-gallery spacing of MMT facilitates the entry of the polymer matrix molecules into the galleries, as the hydrophilic MMT surface changed to an organophilic surface.

Modified pastes

Change of color

Lightness (L):* The data obtained from color change measurements were listed in table 2 and 3. Generally, it was clear that lightness of all pastes decreased with increasing thermal aging time. In the case of paraloid 82, pastes with mMMT (pastes 5, 6) showed slightly lower lightness compared with the corresponding pastes without mMMT (no.3, 4), but lightness of pastes with mMMT decrease with lower percentage compared to others with no mMMT. Pastes with $CaCO_3$ as filler recorded higher lightness than that with microballones and decrease with higher percentage with thermal ageing time.

n the opposite, it was observed that for paraloid 72 pastes with $CaCO_3$ exhibit lower lightness than that with microballons. And that with clay recorded slightly higher lightness than others with no clay as measured in the previous search but still decrease with lower percentage [31].

Red – green color (a):* It was noted from Tables 2 & 3 that the values obtained were in green color for all pastes (the results were minus). And the value (green color) slightly decreased with increasing the ageing time for all pastes.

Yellow – blue color (b):* The data obtained shows that the yellow color slightly increased with increasing the ageing time with all pastes studied.

Total color difference (ΔE): Generally, it could be concluded from Tables 2 & 3 that the color changes with thermal ageing for all pastes [40-42]. Colors became highly variable with the time exposure to high temperatures that may be explained that the heat exposure causes chemical and mechanical changes to materials that result in discoloration [43, 44].

But pastes with MMT/polymer nanocomposite as adhesive either paraolid 72 or 82 were the highest resistant to colour change with thermal ageing in which the changes were with negligible values, by comparing pastes no. 3, 4 with pastes no. 5, 6. Also, comparing pastes no. 1, 2 with others obtained in our previous work without MMT [31], we find that the presence of MMT nanocomposite caused increasing the lightness and increase the color resistance against thermal ageing.

In addition, pastes with micro-ballons as filler no. 2, 4 ,6 are more resistant to colour change with thermal ageing compared with pastes with $CaCO_3$ filler pastes no. 1, 3, 5. So, it was noted that paste no. 3 was with the highest color changes and followed by pastes 1, 5, 4, 2 and the lowest change was obtained from the paste 6.

It was common that one of the most important guidelines for the material used in conservation must not alter so as to affect the object physically or chemically, and should have a long service life [45]. So, the addition of modified MMT as nanoclay could provide indirect protection against the deleterious effect of weathering, resulting in less lightening [46]. According to Horie and Eshraghi et al. [47, 48] paste no. 6 with MMT/paraolid 82 is the highest resistant followed by pastes 2, 4, 5, 1 and the highest changes was obtained from the paste no. 3.

Fourier Transform Infrared Spectroscopy (FTIR)

IR spectra of the pastes before and after ageing were presented in Figure 5 to show the effect of thermal aging on the structure of pastes with and without MMT. For paste no. 1, it was noted that absorption of Calcium Carbonate after ageing was very close to that before ageing indicating the stability of Calcium Carbonate during ageing process. For paraloid 72, C-H stretching bands didn't change at 2924.5 cm^{-1}. C=O stretching bands shifted to little high value from 1737.6 to 1739.5 cm^{-1} and its intensity increased after thermal ageing due to oxidation effect. C-O stretching bands were shifted to lower value from 1129.1 to 1108.9 cm^{-1}. O-H and Si-O stretching bands in montmorillonite clay (MMT) didn't change after ageing.

TABLE 1: XRD Data Obtained for the neat MMT and the modified MMT

	2θ	d-space nm
Neat MMT	6.5064	13.5
Modified MMT	6.2465	14.54

TABLE 2: Color changes of pastes No. 1, 2 studied before and after heat ageing

Samples	Ageing days	Paste (1) Color changes				Paste (2) Color changes			
		L*	a*	b*	ΔE	L*	a*	b*	ΔE
1	0	87.76	-0.3	1.36	—	95.84	-0.25	0.44	—
2	1	87.84	-0.3	1.91	0.55	95.79	-0.25	0.44	0.05
3	2	86.98	-0.29	1.94	0.97	95.61	-0.25	0.45	0.23
4	3	86.25	-0.29	1.99	1.63	95.57	-0.24	0.45	0.27
5	4	86.1	-0.29	1.99	1.77	95.47	-0.24	0.46	0.37
6	5	86.08	-0.28	1.99	1.79	95.26	-0.24	0.46	0.58
7	6	85.51	-0.28	2	2.33	95.01	-0.23	0.47	0.83
8	7	85.32	-0.27	2.03	2.52	94.83	-0.23	0.47	1.0.1
9	8	84.93	-0.27	2.05	2.91	94.57	-0.23	0.47	1.27

TABLE 3: Color changes of pastes No. 3, 4, 5 and 6 studied before and after heat ageing

Samples	Ageing days	Paste (3) Color changes				Paste (4) Color changes				Paste (5) Color changes				Paste (6) Color changes			
		L*	a*	b*	ΔE	L*	a*	b*	ΔE	L*	a*	b*	ΔE	L*	a*	b*	ΔE
1	0	95.66	-0.21	1.47	—	93.54	-0.32	1.34	—	94.63	-0.35	2.32	—	93.18	-0.15	1.4	—
2	1	95.32	-0.2	1.52	0.34	93.44	-0.31	1.46	0.15	94.26	-0.34	2.4	0.37	93.09	-0.15	1.61	0.24
3	2	95.2	-0.19	1.6	0.48	92.83	-0.3	1.58	0.74	93.94	-0.32	2.52	0.71	92.97	-0.14	1.75	0.41
4	3	94.45	-0.19	1.6	1.22	92.52	-0.29	1.65	1.06	93.49	-0.32	2.57	1.17	92.87	-0.14	1.88	0.58
5	4	93.99	-0.18	1.62	1.68	92.2	-0.27	1.76	1.41	93.06	-0.31	2.61	1.6	92.73	-0.14	1.9	0.67
6	5	93.85	-0.18	1.7	1.83	92.02	-0.27	1.84	1.6	92.95	-0.31	2.63	1.71	92.63	-0.12	1.96	0.79
7	6	93.4	-0.17	1.72	2.27	91.97	-0.26	1.92	1.67	92.67	-0.3	2.68	1.99	92.56	-0.12	2.02	0.88
8	7	93.28	-0.17	1.74	2.4	91.96	-0.25	2.04	1.72	92.39	-0.27	2.78	2.29	92.54	-0.12	2.02	0.89
9	8	92.8	-0.17	1.85	2.89	91.94	-0.24	2.48	1.96	92.15	-0.27	2.82	2.53	92.54	-0.1	2.09	0.94

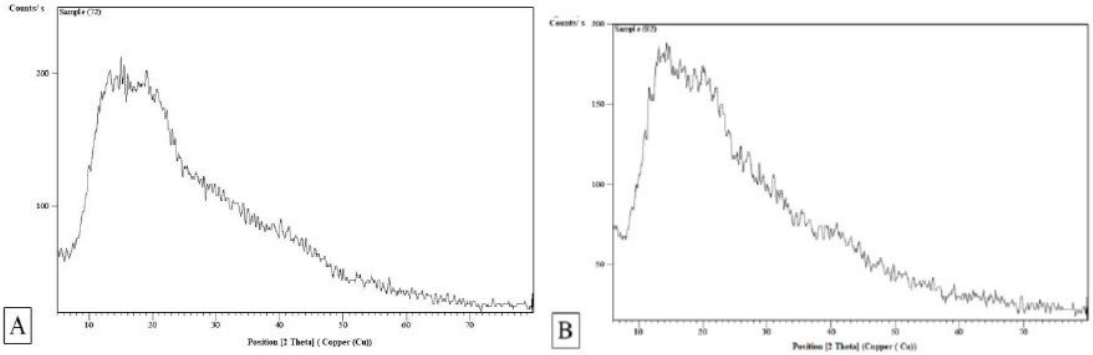

Figure 4: XRD patterns for MMT/ Paraloid 72 (A) and MMT/ Paraloid 82 (B) nanocomposites

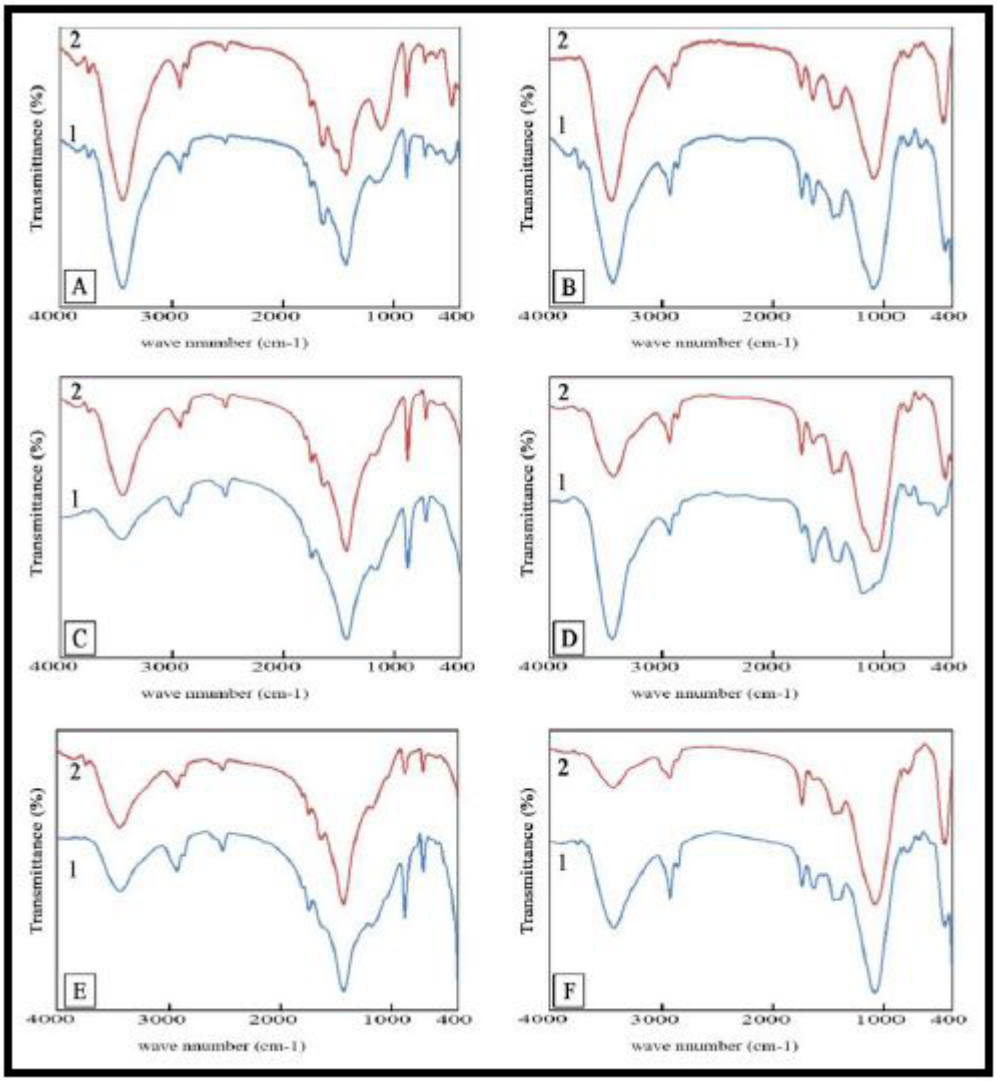

Figure 5: FTIR spectra of pastes before (1) and after ageing (2): (A) paste no. 1; (B) paste no.2; (C) paste no. 3; (D) paste no. 4; (E) paste no.5; (F) paste no. 6

Paste no.2, Glass micro-balloon Si-O-Si stretching band shifted to lower value from 1093.4 to 1085.7 cm^{-1}. Paraloid B–72, C-H stretching bands shifted to high value from 2924.5 to 2927.4 cm^{-1}. C=O stretching bands shifted to little lower value from 1737.6 to 1736.6 cm^{-1}. O-H stretching bands for MMT didn't change, but its intensity decreased after thermal ageing due to loss of water.

Paste no.3, for paraloid B-82, C-H stretching band shifted to lower value after ageing from 2929.3 to 2925.5 cm^{-1}. C=O stretching bands shifted to little high value from 1736.6 to 1737.6 cm^{-1}. C-O stretching bands shifted to higher value from 1161.9 to 1172.5 cm^{-1} and a new band appeared after thermal ageing at 1627.6 cm^{-1} due to oxidation.

Paste no.4, for Glass micro-balloon Si-O-Si stretching band after ageing shifted to very high value from 1042.3 to 1081.9 cm^{-1}. For paraloid B–82, C-H stretching bands didn't change at 2925.5, C=O stretching bands shifted to high value from 1732.7 to 1735.6 cm^{-1} and its intensity increased after thermal ageing due to oxidation effect. C-H bending bands shifted to very high value from 1427.1 to 1447.3 cm^{-1}, Peaks before ageing between 1182.2 to 1042.3 cm^{-1} broader than that after ageing

Paste (5): paraloid B-82, C-H stretching bands didn't change at 2925.5, C=O stretching bands shifted to higher value from 1734.7 to 1737.6 cm^{-1}, C-O stretching bands shifted to high value from 1169.6 to 1172.5 cm^{-1}. Peaks before ageing between 1734.7 to 1169.6 cm^{-1} completely changed after ageing. For MMT, O-H stretching bands shifted from 3441.4 to 3437.5 cm^{-1} and its intensity increased after thermal ageing due to oxidation effect.

Paste (6): for glass micro-balloon Si-O-Si stretching band didn't change after ageing at 1079.9 cm^{-1}; it means that there is stability for glass micro balloons after modification by nano MMT clay. Paraloid B-82, C-H stretching bands shifted to high value from 2924.5 to 2929.3 cm^{-1}, C=O stretching bands didn't change value and its intensity decreased after thermal ageing due to loss of water. For MMT, O-H stretching bands after ageing were shifted to high value from 3431.7 to 3438.5 cm^{-1} and its intensity decreased after thermal ageing due to loss of water.[49,50].

Tensile and Elongation measurements:

Tensile strength:

Data obtained are represented in Figure (6 A) and it was observed that, generally, tensile strength decreased with increasing aging time for all pastes studied but with variable values and it could be attributed to that accelerated thermal aging processes produced weak molecules and increased brittleness [51, 52]. The data in details show that before ageing, tensile strength of pastes no. 1, 3, 5 are with higher value than pastes no. 2, 4, 6, respectively, while the tensile strength of the first group decrease with ageing faster than second group. Ex., at 100°C after 8 days of exposure, the tensile strength decreased in paste no.1 by 54% and in paste no. 2 by 45%. Also, the tensile strength decreased in paste no.3 by 52% and in paste no. 4 by 45%. The tensile strength decreased in paste no.5 by 44% and in paste no. 6 by 30% . It was observed that pastes with clay showed resistance to the decay of the tensile with ageing time.[53]

Elongation:

It was clear from the data obtained (Figure 6 B) that, generally, elongation decreased with aging time for all pastes studied. It was noted that before ageing, elongation of pastes no. 1, 3, 5 are with higher value than pastes no. 2, 4, 6, respectively. While elongation values of the first group those with $CaCO_3$ decrease with ageing faster than second group those with microballons. Ex., at 100°C after 8 days of exposure, the elongation decreased in paste no.1 by 48% and in paste no. 2 by 37%, in paste no.3 by 57% , in paste no. 4 by 42% , in paste no.5 by 43% and in paste no. 6 by 29%. It was noted that pastes with modified MMT enhance the mechanical properties of pastes with respect to those with no mMMT. [53]

According to results above, the presence of montmorillonite as mMMT/polymer nanocomposite enhanced the physico-mechanical properties of polymer and resist their decay over thermal aging [54-58].

Compressive strength

The data obtained are represented in Figure (6 C) that show, generally, the decrease of compressive strength with increasing aging time for all pastes studied. Compressive strengths of pastes no. 1, 3, 5 are with higher value than pastes no. 2, 4, 6,

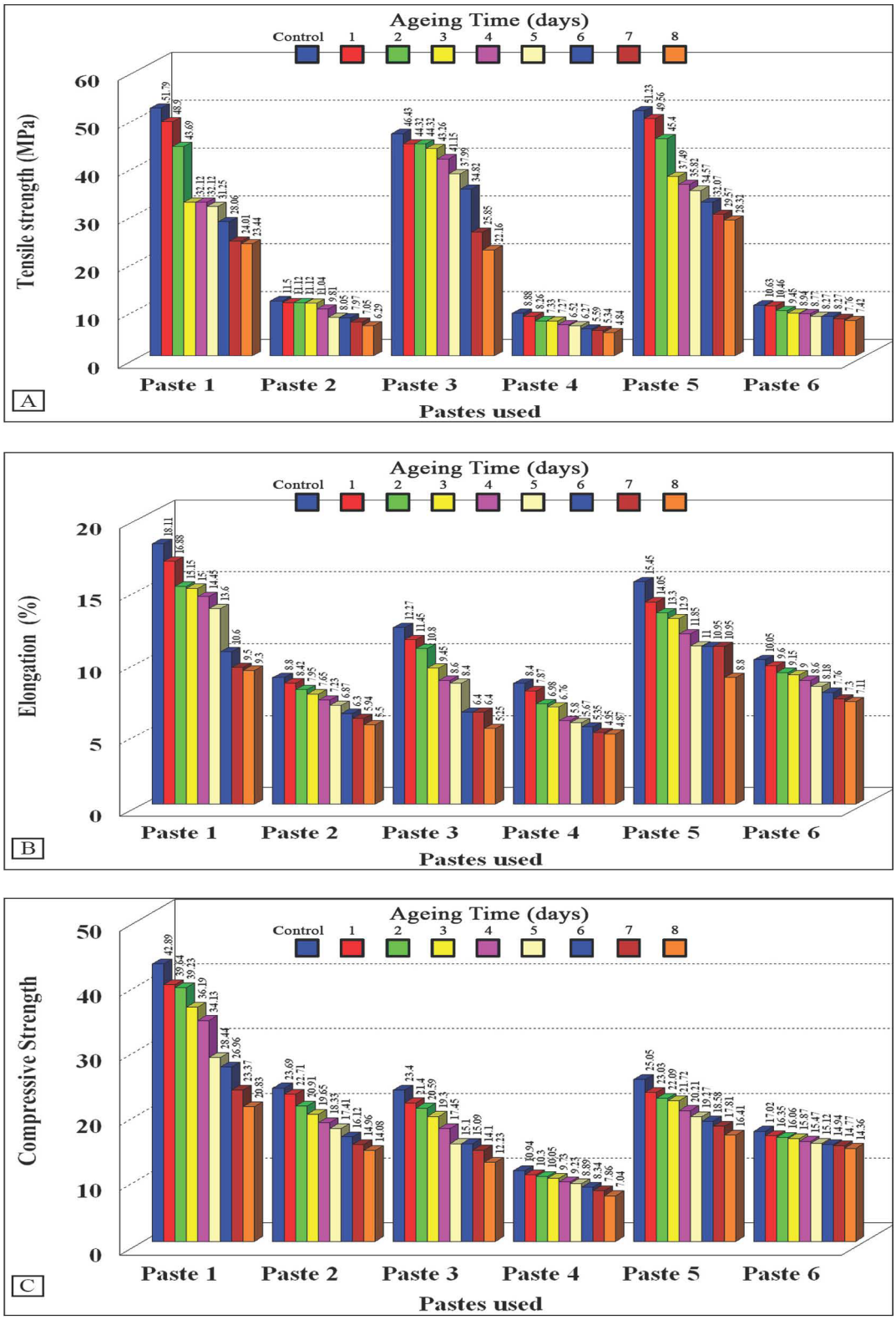

Figure 6: (A) Tensile strength, (B) Elongation and (C) Compressive Strength

respectively. While, compressive strength of the first group decreased faster than that of second group. Ex., the compressive strength decreased in paste no.1 by 51%, in paste 2 by 40%, in paste no.3 by 47% and in paste no. 4 by 35%. also, the reduction in compressive strength decreased in paste no.5 by 34% and in paste no. 6 by only 15% after 8 days of exposure at 100 °C.

It could be concluded that generally there is a considerable reduction in compressive strength with ageing [56] that may be attributed to that long term exposure to elevated temperatures resulted in loss of water leading to a decrease in compressive strength resistance [59]. On the other hand, pastes involved mMMT/polymer nanocomposite suggested excellent compressive strength resistance specially paraloid 82 (paste 6 has the most compressive strength resistance) where pastes with low compressive strength are required for completion and filling cracks processes [60]. So, the addition of mMMT enhance the properties of pastes such as stiffness, hardness and aging resistance [7].

Investigation of the surface morphology by SEM:

Surface morphology of pastes were investigated using the scanning electron microscope to provide more details about the state of the surface before and after ageing process. It could be concluded that the representative SEM images (Figure 7) could show that high temperature aging relaxes the intrinsic molecular stresses also degradation of materials at elevated temperatures are predominantly responsible for the surface effect and contribute to the deterioration of the mechanical properties under impact conditions [61]. Also, leads to a structural reconfiguration and promote changes in surface morphology. The aging mechanism responsible for the deformation and loss of sample surface [62- 64].

It was clear from pastes no. 1, 3, 5 before ageing (A images) those with calcium carbonate as filler participate with cubic morphology. The crystal of calcium carbonate was distributed between the nanocomposite molecules and covered all the surface parallel with polymer composite. The thermal ageing resulted in some destruction of calcium carbonate and nanocomposite as shown in (B images) and the surface became coarse and some gaps were formed. It was noted that paste 5 showed the lowest coarse and little gaps on the surface. While, paste 3 that doesn't involve mMMT showed the highest influence for thermal ageing where its effect on paraloid B 82 was higher than its effect on calcium carbonate. Where, random distribution of calcium carbonate hence lots of gaps were observed on the surface..

It was observed from pastes no. 2, 4, 6 before ageing (A images) those with micro-balloon participate as filler, there is good distribution of micro-balloon spheres and covered with the mMMT nanocomposite for pastes 2,6 or polymer for paste 4 and cohered them together. The thermal ageing resulted in some destruction for micro-balloon spheres that broken (B images), while, nanocomposite cohered them was not affected.

But paste no. 4, that without mMMT, was the most influenced by the thermal ageing where, more paraloid B. 82 layers covered the surface of micro-balloon spheres were flaked and more of micro-balloon spheres were broken. In the opposite, paste no, 6 showed very low effect of accelerated heat ageing and very little of micro-balloon spheres were broken (6B image). Indicating that mMMT improved interfacial bonding between nanoclay and polymer [7].

Contact angle (wettability)

The images and values of contact angles on pastes' samples were tabulated (Table 4). Generally, it was shown that the contact angle values of the pastes were varied with ageing time where its value decreased with the time. This means that the wettability increased with increasing the ageing time. However, they varied by different ratio, it was shown that the increase in contact angle hence the hydrophobicity is mainly attributed to the difference in both the chemical properties of polymer surface and its surface morphology.

When comparing pastes no.1 and 2 with reduction in contact angle as 18.3% and 9.2% with their corresponding samples in the previous paper [31] 29% for paste 1 without mMMT and 12.2% for paste 2 without mMMT. And comparing pastes 5 and 6 with reduction in contact angle as 12% and 7.5% with their corresponding pastes without mMMT paste 3 (22%) and paste 4 (11%), respectively. It was observed that pastes that contain the modified MMT/ paraloid nanocomposite (pastes 2, 6) are with, somewhat, time-independent contact angle in comparison to other pastes in absence of mMMT. Where the modified MMT is responsible for increasing the

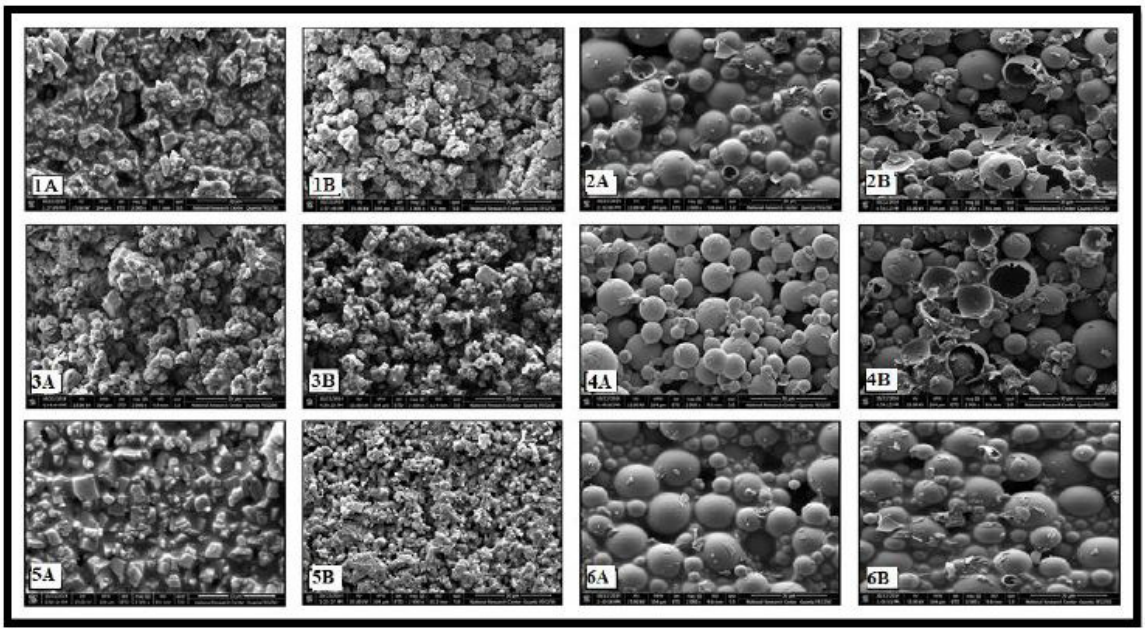

Figure 7: Scanning electron micrographs of pastes (1-6) used; (A) the paste before ageing and (B) the paste after ageing.

hydrophobicity of the paste [65]. Also, it was noted that pastes with micro-balloons as filler (pastes no.2, 4, 6) showed much lower ratio of reduction than their corresponding pastes (1, 3, 5) that contain $CaCO_3$ filler. The reduction in the contact angle value after 8 days of heat ageing was calculated for each sample and they were 18.3% , 22% and 12% for pastes 1, 3 and 5 respectively. 9.2%, 11% and 7.5% for pastes 2, 4 and 6 respectively. Jose, A. J. and Alagar, M. [66] proved that the raise in contact angle value or the hydrophobicity is related with the surface roughness that can be resulted from the addition of modified clay or from the nature of microballone with respect to $CaCO_3$.

Density, porosity and water absorption

Density

It was clear from the data obtained from density measurement (Table 5) that the paste no. 5 recorded the highest density, followed by pastes no. 1, 3, 6, 4, 2 consequently. So, samples with clay and $CaCO_3$ component recorded highest value of density with respect to samples with microballons component. Generally, it was noticed that the density decreased with increasing thermal ageing time. The reduction in density of pastes after 8 days of thermal ageing was calculated as 3.3% for paste no. 1, 2.4% for paste 2 (the corresponding pastes without clay recorded a reduction as 8.6% and 2.6% , respectively) [31], 2.7% for paste 3, 2.2% for paste 4, 1.8% for paste 5, and 0.8% for paste 6. It could be noted that samples with clay enhance more resistant to decay of density with thermal ageing.[67]

Porosity

The data obtained from porosity measurement showed that paste no. 1 recorded the highest value of porosity, followed by paste 3, 5, 4, 2 and 6 consequently. Generally, the porosity increased with increasing the thermal ageing time. The increasing in the porosity of pastes used after 8 days of thermal ageing were calculated as 69.7% for paste no. 1, 53.3% for the paste No. 2 (the corresponding pastes without clay recorded an increase as106% and 62.8% , respectively), [31] 65% for paste no. 3, 56.3% for paste no. 4, 32% for paste no. 5, and 27.3% for paste no. 6. It could be concluded that samples with clay exhibit lower porosity values and more resistance against time of thermal ageing.

Water absorption

It was clear from Water absorption measurement that paste no. 1 recorded the highest water absorption followed by paste 3, 2, 4, 5 and 6 consequently. Generally, Water absorption increased with increasing the thermal ageing time. The percentage of increasing the water absorption of pastes after 8 days of thermal ageing was 93.4% for paste no. 1, 56% for paste 2, (corresponding to 125.5% and 67% for the same pastes with no clay, respectively) [31], 60.4% for paste 3, 42.3% for paste 4, 38.6% for paste 5, and 32% for paste 6. It was noted that the incorporation the modified MMT increase the hydrophobicity of pastes and hence could reduce the water absorption and increase its sustainability against the thermal ageing time. [67]

Conclusion

It can be concluded that employing modified MMT with paraloid 72 or 82 as nanocomposite and their using as adhesive in filling pastes with glass microballoon filler enhanced their chemical and physical properties and achieved high thermal ageing resistance. Where, the presence of mMMT exhibited a good resistance against thermal ageing with the negligible change of color and high stability, it has the lowest change value in mechanical properties and there is almost no change in the surface morphology before and after exposure to thermal ageing with respect to pastes with no mMMT. Moreover, samples with mMMT enhanced the highest value of contact angle and density and are more resist to the reduction with ageing time, however, are with the lowest porosity and water absorption values and are more resist for raising over ageing. These may be due to the interfacial layered bonding between polymer and mMMT improve thermal resistance and improve outstanding mechanical performance

TABLE 4: Values of contact angle (wettability) for studied pastes samples before and after accelerated heat ageing

samples	Ageing time (days)	Paste (1)		Paste (2)		Paste (3)		Paste (4)		Paste (5)		Paste (6)	
		Contact Angle	Value	Contact Angle	Value	Contact Angle	Value	Contact Angle	Value	Contact Angle	Val-ue	Contact Angle	Value
1	0		**120°**		**130°**		**122°**		**131°**	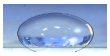	**126°**		**133°**
2	1		**117°**		**130°**		**120°**		**131°**	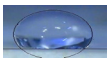	**124°**		**132°**
3	2		**115°**		**129°**		**118°**		**130°**	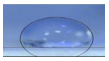	**123°**		**131°**
4	3		**112°**		**128°**		**115°**		**129°**		**120°**		**129°**
5	4		**109°**		**126°**		**111°**	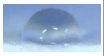	**128°**		**118°**		**128°**
6	5		**107°**		**124°**		**108°**		**127°**	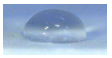	**116°**		**126°**
7	6		**103°**		**121°**		**102°**		**125°**	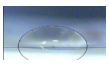	**115°**		**125°**
8	7	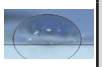	**102°**		**120°**		**99°**	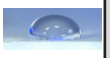	**121°**		**113°**		**124°**
9	8	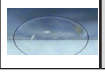	**98°**		**118°**		**95°**	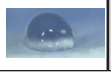	**117°**		**111°**		**123°**

TABLE 5:Density, porosity and water absorption of pastes studied before and after heat ageing

Ageing time (days)	Paste (1)			Paste (2)			Paste (3)			Paste (4)			Paste (5)			Paste (6)		
	Density g/cm^3	Porosity (%)	Water absorption (%)	Density g/cm^3	Porosity (%)	Water absorption (%)	Density g/cm^3	Porosity (%)	Water absorp-tion (%)	Density g/cm^3	Porosity (%)	Water absorption (%)	Density g/cm^3	Porosity (%)	Water absorption (%)	Density g/cm^3	Porosity (%)	Water absorption (%)
0	0.78	16.5	11.15	0.289	1.5	7.34	0.74	8	10.81	0.292	1.6	6.15	0.82	4.8	8.44	0.294	1.1	4.34
1	0.78	17.5	13.42	0.2875	1.6	7.89	0.735	9.6	11.29	0.2915	1.7	6.53	0.82	4.9	8.66	0.2935	1.15	4.75
2	0.77	19	14.97	0.286	1.7	8.42	0.73	10.5	12.44	0.29	1.8	6.89	0.815	5.05	8.91	0.2935	1.2	4.92
3	0.765	20.7	16	0.2845	1.8	8.9	0.73	11.2	13.72	0.289	1.85	7.18	0.815	5.2	9.22	0.293	1.2	5.07
4	0.765	22	17.88	0.284	1.9	9.56	0.725	11.7	14.92	0.2885	1.9	7.33	0.81	5.4	9.87	0.2925	1.25	5.23
5	0.76	24	18.3	0.2835	2	10.3	0.725	12.3	15.87	0.2875	2	7.72	0.81	5.7	10.14	0.2925	1.3	5.41
6	0.76	25.4	29.63	0.283	2.1	10.88	0.725	12.6	16.24	0.2865	2.05	8	0.805	6	10.56	0.292	1.35	5.58
7	0.76	27	20.77	0.2825	2.2	11.15	0.72	13	16.93	0.286	2.25	8.23	0.805	6.1	11	0.292	1.35	5.67
8	0.755	28	21.56	0.282	2.3	11.46	0.72	13.2	17.34	0.2855	2.5	8.76	0.805	6.3	11.7	0.2915	1.4	5.73

References

1. Ghosh A., Nano-Clay Particle as Textile Coating. *International Journal of Engineering & Technology*, **11** (5), 40 – 43(2011).

2. Mahdi L. M. J., Muniandy R., Yunus R. B., Hasham S. and Aburkaba E., Effect of Short Term Aging on Organic Montmorillonite Nanoclay Modified Asphalt. *Indian Journal of Science and Technology*, **6** (11), 5434–5442 (2013).

3. You Z., Mills-Bee J., Foley J. M., Roy S., Odegard G. M., Dai Q. and Goh S. W., Nanoclay-modified asphalt materials: preparation and characterization. *Journal of Construction and Building Materials*, **25** (2) 1072–1078 (2010).

4. Galooyak S. S., Dabir B., Nazarbeygi A. E. and Moeini A., Rheological properties and storage stability of bitumen/SBS/montmorillonite composites. *Journal of Construction and Building Materials*, **24** (3) 300–307 (2010).

5. Yu J., Zeng X., Wu S., Wang L. and Liu G., Preparation and properties of montmorillonite modified asphalts. *Journal of Materials Science and Engineering*, **447** (1) 233–238 (2007).

6. Yu J., Wang X., Hu L. and Tao Y., Effect of various organo modified montmorillonites on the properties of montmorillonite/bitumen nanocomposites. *Journal of Materials in Civil Engineering*, **22** (8) 788–793 (2010).

7. Sharma P. K., Upadhyaya P. and Chand N. Effect of Heat aging on Mechanical Performance of MMT Clay Reinforced Thermoplastic Polyurethane (TPU)/EPDM Rubber Blends based Nano Composite. *European Journal of Advances in Engineering and Technology*, **2** (5) 23-26 (2015).

8. Pavlidou S. and Papaspyrides C. D., A Review on Polymer–Layered Silicate Nanocomposites. *Journal of Progress in Polymer Science*, **33** (12), 1119–1198 (2008).

9. Gilman J. W., Flammability and Thermal Stability Studies of Polymer Layered Silicate (clay) Nanocomposites. *Journal of Applied Clay Science*, **15** (1/2), 31–49 (1999).

10. Saadat-Monfared A., Mohseni M. and Tabatabaei H. M., Polyurethane Nanocomposite Films Containing Nano Cerium Oxide as UV Absorber, Part 1, Static and Dynamic Light Scattering, Small Angle Neutron Scattering and Optical Studies. *Journal of Colloids and Surfaces A*, **408**, 64–70 (2012).

11. Pashaei S., Hatna S. and Syed A. A., Investigation on Thermal, Mechanical and Morphological Behaviours of Organo Nanoclay Incorporated Epoxy Nanocomposites. *Journal of Engineering and Applied Sciences*, **5** (12), 76-86 (2010).

12. Barua S., Gogol S., Khan R. and Karak N., *Silicon-based nanomaterials and their polymer nanocomposites*, ch. 8, nanomaterials and polymer nanocomposites Elesveir Inc., p 261-305 (2019).

13. Abdel-Maksoud G., Comparison between the Properties of "Accelerated Aged" bones and archaeological bones. *Journal of Mediterranean Archaeology and Archaeometry*, **10** (1), 89–112 (2010).

14. Pestle W.J., Colvard M., Bone collagen preservation in the tropics: a case study from ancient Puerto Rico, J. Archaeol. Sci. **39** (7), 2079-2090 (2012).

15. Barth H.D., Zimmermann E.A., Schaible E., Tang S.Y., Alliston T. and Ritchie R.O., Characterization of the effects of X-ray irradiation on the hierarchical structure and mechanical properties of human cortical bone, Biomaterials **32** (34), 8892–8904 (2011).

16. Walker G.T., The chemical and microbial degradation of bones and teeth,ch 1, Adv. Human Paleopathol. Publisher: Wiley, Editors: Ron Pinhasi and Simon Mays (2008) 3–30.

17. Wyszecki G. and Stiles W. S. *Color Science Concepts and Methods. Quantitative Data and Formulae*. Second Edition, JohnWiley & Sons, Inc. New York (2000).

18. Fuchs R. K., Allen M. R., Ruppel M. E., Diab T., Phipps R. J., Miller L. M. and Burr D. B., In situ examination of the time-course for secondary mineralization of Haversian bone using synchrotron Fourier transform infrared micro spectroscopy. *Journal of Matrix Biology*, **27** (1), 34-41 (2008).

19. Nielsen-Marsh C.M. and Mhedges R. E., Patterns of diagenesis in bone I: the effects of site environments, *Journal of Archaeological Science,* **27**(12), 1139-1150 (2000).

20. Hamilton D. L. Basic Methods of Conserving Underwater Archaeological Material Culture. *Nautical Archaeology Program, Department of Anthropology*, Texas A&M University, pp. 22 – 24 (1997).

21. Stollman S., Bell M., Denize S., Lutzke B. and Krause D. K., The Conservation Treatment of Canterbury Museum's Blue Whale Skeleton. *Journal of Canterbury Museum*, **19**, 35 – 60 (2005).

22. Effenberger F., Schweizer M. and Mohamed W. S. Synthesis and characterization of some polyacrylate/montmorillonite nanocomposites by in situ emulsion polymerization using redox initiation system. *Journal of Applied Polymer Science*, **112** (3), 1572–1578 (2009).

23. Nguyen Q. T. and Baird D. G., Preparation of Polymer–Clay Nano composites and Their Properties. *journal of Advances in Polymer Technology*, **25** (4), 270–285 (2006).

24. Feller R. L., *Accelerated Ageing, Photochemical and Thermal Aspects*, Research in Conservation, The Getty Conservation Institute (1994).

25. Budrugeac P., Badea E., Gatta G. D., Miu L. and Com˘anescu A., A DSC study of deterioration caused by environmental chemical pollutants to parchment, a collagen-based material. *Journal of Thermochimica Acta*, **500** (1) 51–62 (2010).

26. Arnold R. B., ASTM's Paper Aging Research Program, http://palimpsest.stanford.edu/byauth/arnold/astm-aging-research/cd (2014).

27. Ahmed H. E, Mohamed W.S., Saad H., Nasr H.E., Morsy M., Mahmoud N., Degradation Behavior of Nano-Glue Adhesive due to Historical Textiles Conservation Process, *Egyptian journal of Chemistry.* **60** (6) 1123- 1133 (2017).

28. Vasilache V., Boghian D., Chirculescu A. I., Enea S. C. and Sandu I., Conservation state assessment and the determination of certain archaeometric characteristics for two bronze items from the early hallstatt period. *Journal of Revista de Chimie*, **64** (2) 152-157 (2013).

29. ASTM, D 412-66 T (1967).

30. Rushdy A. M., Wahba W. N., Youssef A. M., Kamel S., Influence of Bleaching Materials on Mechanical and Morphological Properties for Paper Conservation, *Egyptian Journal of Chemistry*, **60** (5) 893 - 903 (2017).

31. Abdel-Maksoud G., Sobh R., Tarek A., Samaha S.H., Evaluation of some pastes used for gap filling of archaeological bones, *Measurement* **128,** 284–294 (2018).

32. Havlínová B., Katuscák S., Petrovicová M., Maková A. and Brezová V. A Study of Mechanical Properties of Papers Exposed to Various Methods of Accelerated Ageing, Part I, The effect of heat and humidity on original wood-pulp papers. *Journal of Cultural Heritage*, **10**, 222–231 (2009).

33. Al-Dosari M.A., Darwish S., Abd El-Hafez M., Elmarzugi N., Al-Mouallimi N. and Mansour S., Effects of adding nanosilica on performance of ethyl silicate (TEOS) as consolidation and protection materials for highly porous artistic stone, *J.Mater.Sci. Eng. A* **6** (7–8), 192–204 (2016).

34. Pinto A.P.F. and Rodrigues J.D., Stone consolidation: the role of treatment procedures, *J. Cult. Herit*. **9**, 38–53 (2008).

35. Jackes M., Sherburne R., Lubell D., Barker Ch.and Wayman M., Destruction of microstructure in archaeological bone: a case study from, *Int. J. Osteoarchaeol.*, **11**, 415–432 (2001).

36. UNI 10859., Cultural Heritage, Natural and Artificial Stones, Determination of Water Absorption by Capillarity, (2000).

37. Al-Dosari M.A., Darwish S.S., Adam M.A., Elmarzugi N.A., Al-Mouallimi N and Ahmed S.M., Ca (OH)2 nanoparticles based on acrylic copolymers for the consolidation and protection of ancient Egypt calcareous stone monuments, *J. Phys. Conf. Ser*. **829** (1), article id. 012009 (2017).

38. Aguzzi C., Cerezo P., Sandri G., Ferrari F., Rossi S., Bonferoni C., Caramella C. and Viseras C., Intercalation of tetracycline into layered clay mineral material for drug delivery purposes, *Journal Materials TechnologyAdvanced Performance Materials*, **29** (2014) - Issue sup3: Part B2: Layered clay biomaterials and human health.

39. Olad A. and Rashidzadeh A., preparation and anticorrosive properties of PANI/NA-MMT and PANI/O-MMT nanocomposites. *Journal of Progress in Organic Coatings*, **62** , 293-298

(2008).

40. Iannuzzi G., Mattsson B. and Rigdah M., Color Changes Due to Thermal Ageing and Artificial Weathering of Pigmented and Textured ABS. *journal of Polymer Engineering and Science*, **53** (8), 1687–1695 (2013).

41. Zanin F. R., Garcia L. F., Casemiro L. A. and Pires-de-Souza F. C., Effect of artificial accelerated aging on color stability and surface roughness of indirect composites. *European Journal of Prosthodontics and Restorative Dentistry*, **16** (1), 10-14 (2008).

42. Evenson J. and Crews P. C., Effects of accelerated heat and light aging on textiles marked with fabric marking pens. *Journal of Textile Specialty Group Postprints*, **4** (13) 23-32 (2004).

43. Janjua A. and Rogers T. L., Bone weathering patterns of metatarsal v. femur and the postmortem interval in Southern Ontario. *International Journal of Forensic Science*, **178** (1) 16-23 (2008).

44. Marín Arroyo A. B., Landete Ruiz M. D., Vidal Bernabeu G., Seva Román R., González Morales M. R. and Straus L. G. Archaeological implications of human-derived manganese coatings: a study of blackened bones in El Miron Cave, Cantabrian Spain. *Journal of Archaeological, Science*, **35** (3), 801-813 (2008).

45. Khoeini M., Bazgir S., Tamizifar T., Nemati A. and Arzani K., Investigation of the modification process and morphology of organosilane modified nanoclay, Ceramics – Silikáty **53** (4), 254-259 (2009).

46. Thompson T. J. Recent advances in the study of burned bone and their implication for forensic anthropology. *International Journal of Forensic Science*, **146**, 203-205 (2004).

47. Horie V., *Materials for Conservation Organic consolidants, Adhesives and Coatings*. Second Edition, pp. 3-4 (2010).

48. Eshraghi A., Khademieslam H., Ghasemi I. and Talaiepoor M., Effect of weathering on the properties of hybrid composite based on polyethylene, woodflour, and nano clay. *Journal of BioResources*, **8** (1), 201-210 (2013).

49. Chen A., Luo Z. and Akbulut M., Supporting Information for: Ionic Liquid Mediated Auto-Templating Assembly of $CaCO_3$-Chitosan Hybrid Nanoboxes and Nanoframes. *Journal of Chemical Communications, the Royal Society of Chemistry*, **47** (8), 2312 - 2314 (2011).

50. Derrick M., Stulik D. and Landry J., *Scientific Tools for Conservation: Infrared Spectroscopy in Conservation Science*. The Getty Conservation Institute, Los Angeles, USA (1999).

51. Hamed G. R. and Zhao J., Tensile behaviour after oxidative aging of gum and black-filled vulcanizates of SBR and NR. *Journal of Rubber Chemistry and Technology*, **72**, 721-730 (1999).

52. Hu X., Li Y., Liu X. and Luo W., *Experimental Studies of Thermal Aging Effects on the Tensile and Tearing Fracture Behavior of Carbon Black Filled Rubbers.* 13th International Conference on Fracture, Beijing, China, 16–21June (2013).

53. El-Sheikhy R., Al-Shamrani M., On the Processing and Properties of Clay/Polymer Nanocomposites CPNC, Lat. Am. j. solids struct. **12** (2), 385-419 (2015).

54. Hassan R. Behavior of Archaeological paper after cleaning by organic solvents under heat accelerated aging. *Journal of Mediterranean Archaeology and Archaeometry*, **15** (3), 141-150 (2015).

55. Ghile D. B., *Effects of nanoclay modification on rheology of bitumen and on performance of asphalt mixtures*. Master thesis, the Delft University of Technology, Netherlands (2006).

56. Ashori A. and Nourbakhsh A., Effects of nanoclay as a reinforcement filler on the physical and mechanical properties of wood based composite. *Journal of Composite Materials*, **43** (18), 1869-1875 (2009).

57. Jahromi S. G. and Khodaii A., Effects of nanoclay on rheological properties of bitumen binder. *Journal of Construction and Building Materials*, **23** (8), 2894–2904 (2009).

58. Lovely K. M. and Chacko A., A Study on strength characteristics of ordinary Portland cement due to storage. *International Journal of Innovative Research in Science, Engineering and Technology*, **2** (3), 612-616 (2013).

59. Fillmore D. L., *Literature review of the effects of radiation and temperature on the aging of concrete*. Idaho National Engineering and

Environmental Laboratory, Bechtel, BWXT Idaho, LLC, September (2004).

60. Barclay R. and Mathias C., An Epoxy/Micro balloon mixture for gap filling in wooden objects. *JAIC*, **28** (1/3), 31 – 42 (1989).

61. Wu S., Wang J. and Jiesheng L., Preparation and fatigue property of nanoclay modified asphalt binder. *International Conference on Mechanic Automation and Control Engineering (MACE)*, pp. 1595-1598 (2010).

62. Cui Z., Ma C. and Lv N., Effects of Heat Treatment on the Mechanical and Thermal Performance of Fabric Used in Firefighter Protective Clothing. *Journal of Fibres & Textiles in Eastern Europe*, **23** (2/110), 74-78 (2015).

63. Todd J., Bruce G., Nguyen K. and Gopinath A., Effect of engine-based thermal aging on surface morphology and performance of Lean NOx Traps. *Journal of Catalysis Today*, **123** (1/4), 285–292 (2007).

64. Karimiyan A., Farhangi H. and Allahyari A. A., *Investigation of the effects of aging on the room and High temperature tensile properties and fracture of Stainless steel 316l weld metal*. 8th International Fracture Conference, Istanbul/ Turkey, 7 – 9 November, 518-526 (2007).

65. Savaş L.A. and Savaş S., Interrelation Between Contact Angle and Interlayer Spacıng of Montmorillonite Clay Used in Polymer Nanocomposıtes. *Polymers & Polymer Composites,* **21** (3), 129-132 (2013).

66. Jose, A. J., & Alagar, M. *Preparation and characterization of polysulfone-based nanocomposites.ch.3,Manufacturing of Nanocomposites with Engineering Plastics, Elsevier Ltd, 31–59* (2015).

67. Malik N., Shrivastava S., Ghosh S. B., Moisture Absorption Behaviour of Biopolymer Polycapralactone (PCL) /Organo Modified Montmorillonite Clay (OMMT) biocomposite films, IOP Conf. Series: *Materials Science and Engineering* 346 (2018) doi:10.1088/1757-899X/346/1/012027

تقييم لمركبات المنتمورولونيت والبوليمر النانوية لملئ فجوات العظام الأثرية

جمعة عبد المقصود[1] , رقية على صبح[2] , أحمد طارق[3]، سماحه سيد حسين[4]

[1] قسم الترميم - كلية الآثار - جامعة القاهرة - الجيزة - مصر.

[2] قسم البلمرات و المخضبات, المركز القومى للبحوث – الدقى – الجيزة – مصر.

[3] مركز الترميم - المتحف المصرى الكبير - وزارة السياحة و الآثار - الجيزة - مصر.

[4] قسم مترولوجيا النسيج - المركز القومي للقياس والمعايرة - شارع ترسا - الجيزة - مصر.

تتعرض العظام الأثرية للعديد من عوامل التلف, لذلك تستخدم البوليمرات لزيادة تحسين خصائصها لتعطي ديمومة اعلي. وقد تم تطبيق وتقييم العجائن التقليدية من قبل. وتهدف هذه الدراسة إلي تقييم بعض العجائن التقليدية المعدلة من أجل تحسينها. لذلك تم تعديل خواص طفلة المنتمورولونيت باستخدام حامض أميني (وقد تم توصيف المنتمورولونيت من خلال مطياف الأشعة تحت الحمراء FTIR و حيود الأشعة السينية XRD، ودراسة المظهر السطحى باستخدام الميكروسكوب الإلكترونى الماسح SEM).

وقد تم عمل عجائن من المركبان النانوية من مادة المنتمورولونيت المعدلة مع البارالويد ب 72(أكريلك بوليمر) وتقييمها من اجل استخدامها لملىء الفجوات واستكمال العظام الأثرية لإعطاء مقاومة اعلي ضد الظروف البيئية المحيطة.

وقد تم عمل تقادم صناعى باستخدام الحرارة لتقييم هذه العجائن، كما تم استخدام بعض أساليب الفحص والتحليل لتقييم بعض الخواص لهذه العجائن مثل التغير اللوني, التحليل بمطياف الأشعة تحت الحمراء (FTIR), قياس الخواص الميكانيكية (قوة الشد ونسبة الاستطالة وقوة الإنضغاط) ودراسة المظهر السطحي باستخدام الميكروسكوب الالكتروني الماسح (SEM).

أكدت النتائج أن العجائن المعدلة مع المنتومورولونيت النانوى أظهرت مقاومة اعلي للتقادم الحراري, وتعطى ثبات اعلي فيما يخص التغير اللوني (حيث أن الاختلاف فى اللون الكلى كان طفيفا بمقدار 0.98) والمظهر السطحي والخواص الميكانيكية. ويشير انخفاض نتائج زاوية التلامس (CONTACT ANGLES) إلي زيادة صلابة السطح. بالإضافة إلي ذلك فقد أظهرت العجائن التي تحتوي علي الطفلة في الصورة النانوية اعلي كثافة, وأعطت مسامية وامتصاص مائى قليل، وأظهرت مقاومة عالية للتقادم الحرارى.